IEEE Access
Multidisciplinary | Rapid Review | Open Access Journal

Received May 14, 2019, accepted May 30, 2019, date of publication June 5, 2019, date of current version June 26, 2019.

Digital Object Identifier 10.1109/ACCESS.2019.2920853

Research on Control Strategy in Giant Magnetostrictive Actuator Based on Lyapunov Stability

XIAOHUI GAO AND YONGGUANG LIU
School of Automation Science and Electrical Engineering, Beihang University, Beijing 100191, China
Corresponding author: Yongguang Liu (lyg@buaa.edu.cn)

This work was supported by the National Natural Science Foundation of China under Grant 11272026 and Grant 11872006.

ABSTRACT The output characteristics of giant magnetostrictive actuator (GMA) are affected by many nonlinear factors, such as hysteresis, load, driving frequency and so on, which would lead to lower positioning precision, poorer repeatability, and even fall into nonlinear instability especially in complex dynamic environment. First, the accurate dynamic mathematical model for GMA is established after analyzing its working principle. Then, the inverse model feed-forward compensation fuzzy PD control based on Lyapunov stability is put forward and applied into the GMA control system. The experiment results indicate that Lyapunov direct method that is integrated into inverse model feed-forward compensation fuzzy PD controller can effectively improve the dynamic output features especially in the complex dynamic environment, reduce the root mean square error from 1.275 to 0.332 and maximum error rate from 26.89% to 7.12%, which not only greatly improve performance and expand the application domain of GMA, but also have very important theoretical significance and high application value in modeling and control approach for some hysteresis systems.

INDEX TERMS Giant magnetostrictive actuator (GMA), Lyapunov, Jiles–Atherton, fuzzy PD.

I. INTRODUCTION

Giant magnetostrictive actuator (GMA) is widely applied in the field of transducer, accurate positioning, active vibration and other dynamic fields [1]–[3] because of its high energy conversion efficiency, large magnetostrictive coefficient and fast dynamic response. But the output characteristics of GMA are affected by many nonlinear factors especially in complex dynamic environment such as high frequency, multi-frequencies, heavy load and so on, which can lead to poor tracking precision and even nonlinear instability [4], [5]. In order to reduce the effect of material hysteresis nonlinearity, the different control algorithms based on the inverse mode are studied and achieve good tracking results [6]–[8] on the low frequency or quasi-static situations. With the development of intelligent control strategies, adaptive control [9], neural network control [10], optimal control [11], [12] are studied to improve the tracking characteristics by constantly adjusting control parameters. They all got good tracking results in the dynamic environment. But, if some improper control parameters are applied in some special circumstances, it may greatly reduce output characteristics and even fall into nonlinear instability especially in the complex dynamic environment. Therefore, how to establish the accurate dynamic mathematical model for GMA, adjust the control parameters based on stability become the key to study the control algorithms, which can reduce the effect of material hysteresis nonlinearity to improve tracking accuracy and avoid falling into the nonlinear instability especially in the complex dynamic environment.

The associate editor coordinating the review of this manuscript and approving it for publication was Ton Do.

II. STABLISHING DYNAMIC MATHEMATICAL MODEL

GMA is shown in Fig.1. It can drive load through giant magnetostrictive material (GMM) rod under the magnetic field produced by the exciting coil and permanent magnet. Pre-pressure is generated by compressing disc springs to increase the magnetostrictive coefficient. Ring permanent magnet can produce bias magnetic field to eliminate the ''double frequency'' characteristic of the GMM and realize the bidirectional displacement output. Top, lower cover and output rod produced by magnetic matter can form a closed

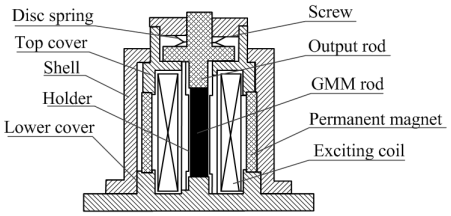

FIGURE 1. GMA.

magnetic circuit with permanent magnet and exciting coil, which can diminish the magnetic leakage and improve the magnetic field environment for GMM rod.

As we all known, memory behaviors of the GMM is non-negligible in the control tasks. The control algorithm based on inverse model can reduce and even eliminate it and improve the controllability. So, how to establish an accurate mathematic model and apply it into real-time control system with lower memory consumption is the key point. Jiles–Atherton (J-A) model has a better description of hysteresis, is easier to be solved and consumes less memory in the control algorithm [13]–[15]. J-A dynamic model was established by Jiles DC and Atherton DL based on domain wall theory to describe internal characteristics of ferromagnetic materials. It has been a relatively mature ferromagnetic hysteresis theory after unceasing amendment and development. The dynamic H-M model of GMM [16]–[19] is given by

$$H_{\mathrm{e}} = H + \alpha M + \frac{9\lambda_s \sigma}{2\mu_0 M_{\mathrm{s}}^2} M \tag{1}$$

$$M_{\mathrm{an}} = M_{\mathrm{s}}(\coth \frac{H_{\mathrm{e}}}{a} - \frac{a}{H_{\mathrm{e}}}) \tag{2}$$

$$M = M_{\mathrm{rev}} + M_{\mathrm{irr}} \tag{3}$$

$$M_{\mathrm{rev}} = c(M_{\mathrm{an}} - M_{\mathrm{irr}}) \tag{4}$$

$$M_{\mathrm{irr}} = (M - cM_{\mathrm{an}})/(1-c) \tag{5}$$

$$M = M_{\mathrm{an}} - k\delta(1-c)\frac{\mathrm{d}M_{\mathrm{irr}}}{\mathrm{d}H_{\mathrm{e}}} - k_1 \frac{\mathrm{d}M}{\mathrm{d}t}\frac{\mathrm{d}M}{\mathrm{d}H_{\mathrm{e}}} - k_2 \left|\frac{\mathrm{d}M}{\mathrm{d}t}\right|^{\frac{1}{2}} \frac{\mathrm{d}M}{\mathrm{d}H_{\mathrm{e}}} \tag{6}$$

where H_{e} is effective magnetic field intensity, H is magnetic field intensity, M is magnetization, α is average field parameters of internal coupling domain, σ is the stress on the GMM rod, M_{s} is saturation magnetization, λ_{s} is saturation magnetostrictive coefficient, μ_0 is permeability of vacuum, M_{an} is magnetization without hysteresis, a is the shape parameter of magnetization without hysteresis, M_{rev} is reversible magnetization, M_{irr} is irreversible magnetization, c is reversible coefficient of losses, k is irreversible coefficient of losses, k_1 is eddy current loss factor, k_2 is abnormal loss factor, δ is direction parameter, when $\mathrm{d}H/\mathrm{d}t > 0$, $\delta = 1$ and when $\mathrm{d}H/\mathrm{d}t > 0$, $\delta = -1$.

According to the working principle, the equivalent mechanical model is given by Fig. 2. The kinetic equation

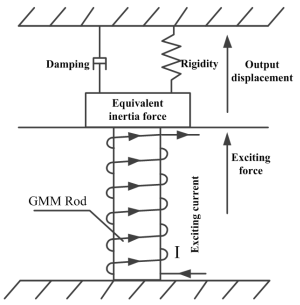

FIGURE 2. Equivalent force model.

of GMA is established based on the Newton second law.

$$F = -\sigma A = M_{\mathrm{e}}\ddot{x} + C_{\mathrm{e}}\dot{x} + k_{\mathrm{d}}x + F_0 \tag{7}$$

$$M_{\mathrm{e}} = \frac{M_M}{3} + M_L \tag{8}$$

where F is the output force of GMA, M_{e} is equivalent mass, C_{e} is equivalent impedance factor of system, F_0 is pre-pressure of dish spring, k_{d} is stiffness coefficient of dish spring, A is cross-sectional area of GMM bar, x is the output displacement of GMA, M_{M} is the mass of GMM rod, M_{L} is mass of the load.

$$x = \varepsilon L \tag{9}$$

where ε, L is respectively the strain and length of GMM bar.

The second-order domain rotation model is shown in (10) [20].

$$\varepsilon = \sigma/E + \gamma_1 M^2 \tag{10}$$

where γ_1 is magnetic elasticity coefficient of GMM rod, and E is elasticity modulus.

According to (7)-(9), the kinetic equation of GMA is established.

$$M_{\mathrm{e}}\ddot{x} + C_{\mathrm{e}}\dot{x} + \frac{EA}{L}x + k_{\mathrm{d}}x + F_0 = \gamma_1 M^2 EA \tag{11}$$

According to the Ampere circuit law considering the magnetic-flux leakage [21], the magnetic field intensity H can be defined as follows:

$$H = H_{\mathrm{bias}} + k_{\mathrm{coil}} I \tag{12}$$

where H_{bias} is bias magnetic field, and k_{coil} is excitation coefficient of the coil with magnetic leakage.

The servo driver can transform control signal to current. The first-order mathematical model can describe its input-output characteristics based on test report provided by the manufacturer (13).

$$\frac{1}{1 + T_d \mathrm{s}} \tag{13}$$

where T_d is the time constant of servo driver.

Therefore, dynamic model mathematical of GMA system can be obtained by combining (1)-(6) with (11)-(13).

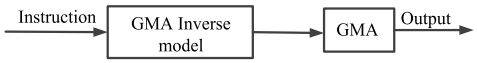

FIGURE 3. Direct inverse model control.

III. RESEARCH ON THE CONTROL STRATEGY

In order to improve GMA performance and increase its application field in the complex dynamic environment. The working principles of the direct inverse model control (DIM), fuzzy PD control (FPD) and inverse model feed-forward compensation fuzzy PD control (FCFPD) are analyzed and introduced. And on this basis the inverse model feed-forward compensation fuzzy PD control based on Lyapunov stability (LFCFPD) is put forward, which applies inverse model feed-forward compensation to reduce the influence of material and structural nonlinearity, fuzzy PD to eliminate the random disturbance, Lyapunov indirect method to guarantee robustness.

A. DIRECT INVERSE MODEL CONTROL

The direct inverse model control (DIM) is directly applied the inverse model into control algorithm which can reduce the effect of hysteresis nonlinearity. The process of solving the inverse model is as following. The desired output displacement instruction x is firstly converted to magnetization M in Eq.11. The relationship between H_e and M is shown in Eq.14 according to Eq.1-6. The effective magnetic field intensity H_e can be solved by fourth order Ronge-Kutta method in Eq.14. When M is increasing, $\delta = 1$ and when M is decreasing, $\delta = -1$. Magnetic field intensity H can be solved by Eq.1 based on H_e and M. Current I is achieved through H according Eq.12. Finally, I is converted to control signal by Eq.13. If the GMA model is sufficient precise, the output of GMA keep highly consistent with instruction.

$$\frac{dH_e}{dM} = \frac{k_1 \frac{dM}{dt} + k_2 \left|\frac{dM}{dt}\right|^{\frac{1}{2}} + k\delta}{M_s(\coth \frac{H_e}{a} - \frac{a}{H_e}) - M + k\delta M_s(\frac{a}{H_e^2} - \frac{1}{a}\mathrm{csch}(\frac{H_e}{a})^2)} \tag{14}$$

B. FUZZY PD CONTROL

Fuzzy control is built on the fuzzy set theory put forward by L.A.Zadeh, which applies fuzzy mathematical language to describe the control law. Since its core concept is to simulate the experiential control based on the dynamic information, it is widely used in the nonlinear systems with strong coupling, time variation and random disturbance. The significant advantage of the fuzzy controller is simple computer language. Whereas some advanced control algorithms, such as neural network and genetic algorithms, require multiple iterations and bulk data processing, they need increase real time control cycle and are not suitable for high frequency dynamic control system. Fuzzy PID controller has the common advantages of fuzzy control and PID control, which can dynamically adjust PID parameters based on current status.

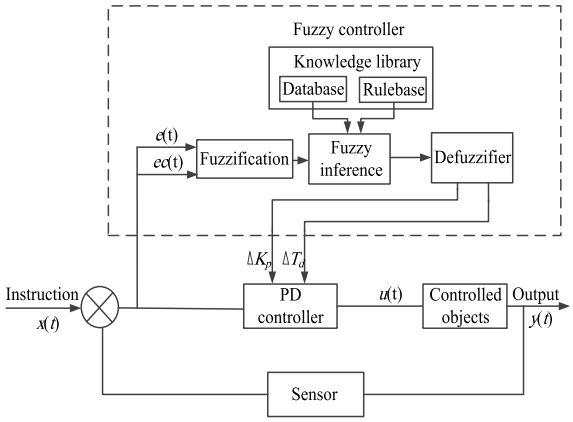

FIGURE 4. Fuzzy PD control.

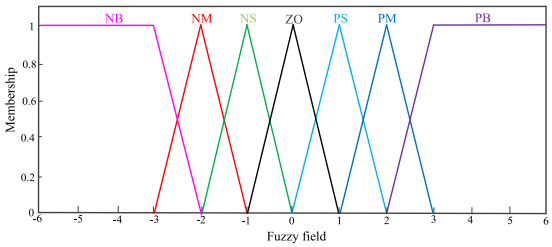

FIGURE 5. Membership function curves.

The I control is mainly used to eliminate static error and cannot receive an evident effect in the high frequency dynamic system [22]. On the contrary, the dynamic tracking accuracy can be affected by the integral saturation.

Fuzzy control is made up of fuzzification, data and rule base, fuzzy inference and defuzzifier, which has many advantages such as strong robustness, high fault tolerance and simple programming language . The fuzzy PD control (FPD) in Fig.4 can get adaptable proportionality and differentiation coefficient according to deviation e and variation of deviation ec [22], [23]. The input of fuzzy PD controller is deviation e and deviation variation ec and its output is ΔK_p and ΔK_d, which is a two-dimensional controller.

$$e = x(k) - y(k) \tag{15}$$

$$ec = e(k) - e(k-1) \tag{16}$$

The membership function is used to describe the subordination relations between element and fuzzy set and ranges from 0∼1. The closer its value is to 1, the higher degree of membership it would have. The fuzzy field e and ec are both [−6,6].The triangular function is applied to define subordinated degree. The membership function curves are shown in Fig. 5 based on the fuzzy field of e and ec.

Where NB is negative big, NM is negative middle, NS is negative small, ZO is zero output, PS is positive small, PM is positive middle, and PS is positive small.

Fuzzy control rules are shown in Tab.1 through debugging.

The value of ΔK_p and ΔK_d can't be achieved directly through fuzzy inferences based on e, ec and fuzzy control rules. The weighted average (17) is applied to get values

TABLE 1. Fuzzy control rules. (a) Fuzzy rules of ΔK_p. (b) Fuzzy rules of ΔK_d.

(a)

ΔK_p / e \ ec	NB	NM	NS	ZO	PS	PM	PB
NB	PB	PB	PB	PB	PS	ZO	NS
NM	PB	PB	PM	PM	ZO	NS	NM
NS	PB	PM	PM	PS	NS	NM	NB
ZO	ZO	ZO	ZO	ZO	ZO	ZO	ZO
PS	NB	NM	NS	PS	PM	PM	PB
PM	NM	NS	ZO	PM	PB	PB	PB
PB	NS	ZO	PS	PB	PB	PB	PB

(b)

ΔK_d / e \ ec	NB	NM	NS	ZO	PS	PM	PB
NB	PB	PB	PB	NB	NB	NM	NS
NM	PB	PB	PM	NM	ZO	PS	PM
NS	PB	PM	PM	NS	PM	PB	PB
ZO	ZO	ZO	ZO	ZO	ZO	ZO	ZO
PS	PB	PB	PM	NS	PM	PM	PB
PM	PM	PS	ZO	ZM	PM	PB	PB
PB	NS	NM	NB	NB	PB	PB	PB

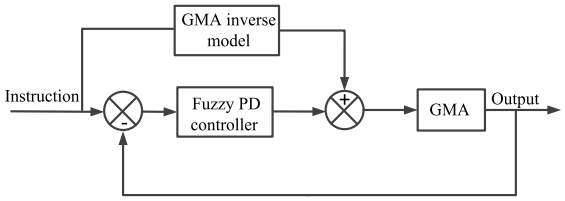

FIGURE 6. Feed-forward compensation fuzzy PD controller.

through defuzzification.

$$x_0 = \frac{\sum_{i=1}^{n} x_i u(i)}{\sum_{i=1}^{n} u(i)} \tag{17}$$

where x_0 is the value of ΔK_p or ΔK_d, x_i is an element in fuzzy inferences, and $u(i)$ is the degree of membership of x_i.

C. INVERSE MODEL FEED-FORWARD COMPENSATION FUZZY PD CONTROL

The working principle of the inverse model feed-forward compensation fuzzy PD controller (FCFPD) is shown in Fig.6, which can apply the inverse model feed-forward compensation to reduce the influence of hysteresis and fuzzy PD controller (FPD) to eliminate random and model error interference.

D. INVERSE MODEL FEED-FORWARD COMPENSATION FUZZY PD CONTROL BASED ON LYAPUNOV STABILITY

Lyapunov stability theory has been a kind of mature theory, which consists of the first Lyapunov method (indirect method) and second Lyapunov method (direct method) [24]. Lyapunov indirect method can determine the stability of the system through solving the state equation. It is very suitable for linear systems and limited for most of nonlinear systems. Lyapunov direct method can determine the stability of system through generating Lyapunov energy equation of system, which has stronger adaptability for most of linear and nonlinear systems.

When state equation is $\dot{X} = f(X, t)$ and $f(X_\mathrm{e}, t) = 0$,

X_e is the equilibrium point of the equation. If X_e is located in the range of spherical domain $B_{\mathrm{R_e}}$ and a scalar function $V(x)$ should be found to meet the following condition:

(1) $V(x)$ exists the first continuous partial derivatives $\dot{V}(x)$.

(2) $V(x)$ is positive definite in the sphere domain $B_{\mathrm{R_e}}$.

(3) $\dot{V}(x)$ is negative definite in the sphere $B_{\mathrm{R_e}}$.

Then, X_e is locally stable. If $\|B_{\mathrm{R_e}}\| \to \infty$, it is global stable.

The transfer function of GMA system can be described as (18) based on (14) through Laplace transform and (13).

$$\mathrm{G}(s) = \frac{\mathrm{Y}(s)}{\mathrm{U}(s)} = \frac{K_\mathrm{a}}{s^3 + a_1 s^2 + a_2 s + a_3} \tag{18}$$

$$K_\mathrm{a} = (\gamma_1 M^2 EA - F_0)/M_\mathrm{e} T_\mathrm{d} \tag{19}$$

$$a_1 = \frac{M_\mathrm{e} + T_d C_\mathrm{e}}{M_\mathrm{e} T_d} \tag{20}$$

$$a_2 = \frac{C_\mathrm{e} L + EAT_d + k_\mathrm{d} T_d L}{M_\mathrm{e} T_d L} \tag{21}$$

$$a_3 = \frac{EA + k_\mathrm{d} L}{M_\mathrm{e} T_\mathrm{d} L} \tag{22}$$

Equation (23) can be obtained by differentiating on both sides of (18).

$$\dddot{y} + a_1 \ddot{y} + a_2 \dot{y} + a_3 y = K_\mathrm{a} u \tag{23}$$

The output u_pd of PD controller can be described by (24).

$$u_\mathrm{pd} = K_\mathrm{p} e + K_\mathrm{d} \dot{e} \tag{24}$$

When instruction is r, system output is y, error is e, controller output is u, PD controller output is u_pd and feed-forward controller output is u_0, the relations among them are as following:

$$e = y - r \tag{25}$$

$$u = u_\mathrm{pd} + u_0 \tag{26}$$

Equation (27) can be obtained by taking the derivative of (25).

$$\begin{cases} \dot{e} = \dot{y} - \dot{r} \\ \ddot{e} = \ddot{y} - \ddot{r} \\ \dddot{e} = \dddot{y} - \dddot{r} \end{cases} \tag{27}$$

E is defined as follows.

$$E = \begin{bmatrix} e & \dot{e} & \ddot{e} \end{bmatrix}^T \tag{28}$$

Equation (29) can be obtained according to (18)∼(28).

$$\dot{E} = \begin{bmatrix} 0 & 1 & 0 \\ 0 & 0 & 1 \\ K_\mathrm{a} K_\mathrm{p} - a_3 & K_\mathrm{a} K_\mathrm{d} - a_2 & -a_1 \end{bmatrix} E \tag{29}$$

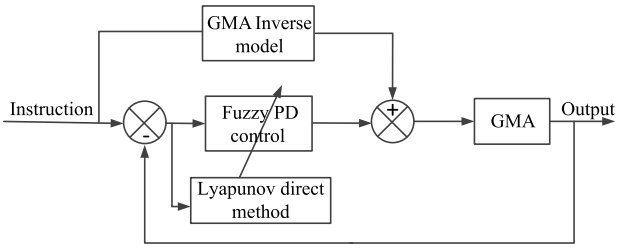

FIGURE 7. Inverse model feed-forward fuzzy control based on Lyapunov stability.

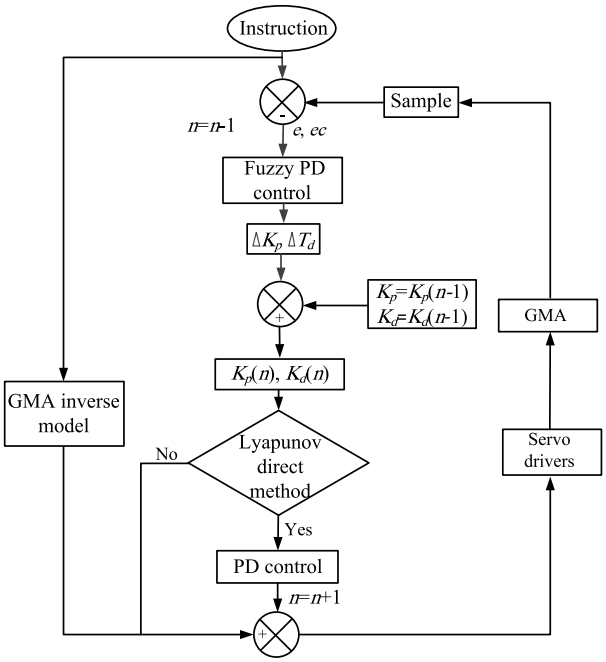

FIGURE 8. Working principle of controller.

The state space equation is shown as follow.

$$\dot{E} = \mathrm{A}E \tag{30}$$

$$A = \begin{bmatrix} 0 & 1 & 0 \\ 0 & 0 & 1 \\ K_\mathrm{a}K_\mathrm{p} - a_3 & K_\mathrm{a}K_\mathrm{d} - a_2 & -a_1 \end{bmatrix} \tag{31}$$

Lyapunov energy function can be defined as (29).

$$V(e) = E^T E \tag{32}$$

If system is stable, $\dot{V}(e) < 0$

$$\dot{V}(e) = \dot{E}^\mathrm{T}E + E^\mathrm{T}\dot{E} < 0 \tag{33}$$

Therefore, K_p and K_d of fuzzy PD control can be taken intoe (33) to calculate $\dot{V}$ (e) If $\dot{V}(e) < 0$, this group of PD parameters is adopted, if $\dot{V}(e) > 0$, it is abandoned and only the inverse model control is adopted.

Fig.7 shows the inverse model feed-forward fuzzy control based on Lyapunov stability (LFCFPD), which apply the Lyapunov stability theory into the FCFPD. The working principle of the LFCFPD is shown in Fig.8.

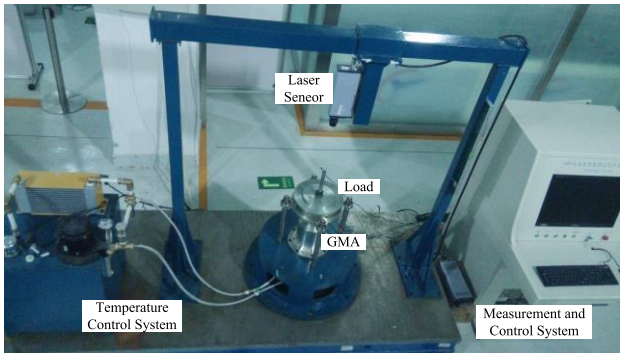

FIGURE 9. GMA test bed.

TABLE 2. GMA model parameters.

Parameter	Value	Parameter	Value
M_s	380769A/m	a	47704A/m
k	22643 A/m	c	0.1
k_1	5.89×10-5	k_2	0.312
μ_0	$4\pi \times 10^{-7}$ N / A^2	H_{bias}	62669.6A/m
γ_1	1.07×10-14	A	3.14cm^2
T_d	1.75×10-4	C_e	30200Ns/m
α	0.417	k_{coil}	16492m-1
E	30Gpa	λ_s	1500ppm
L	0.1m	F_0	1884N
M_M	291g	k_d	1587N/mm

IV. EXPERIMENT RESEARCH

GMA test bed (Fig.9) is applied to do verification experiment for the model and control strategy. It is mainly composed of GMA, laser displacement sensor, temperature control system and measurement and control system. LabWindows and RTX are used for upper and lower computer respectively and sampling period is 0.5ms. The V100-MS high precision micro displacement sensor is adopted to test the displacement of GMA. The measuring error of the system is 0.1μm, which is verified by metrology institute. Temperature control system is applied to maintain the stable operating temperature for GMM rod. The load is changed by applying different mass block.

A. MODEL VERIFICATION

The accurate mathematical model of GMA is very important for the feed forward compensation control. So, we need to verify the correctness of GMA model in different experiments. The model parameters are shown in Tab.2 based on parameters identification with modified simulated annealing differential evolution algorithm [25]. The simulation and experiment curves of GMA in different frequency are shown in Fig.10. The good agreement between simulation and experiments prove the effectiveness of this model.

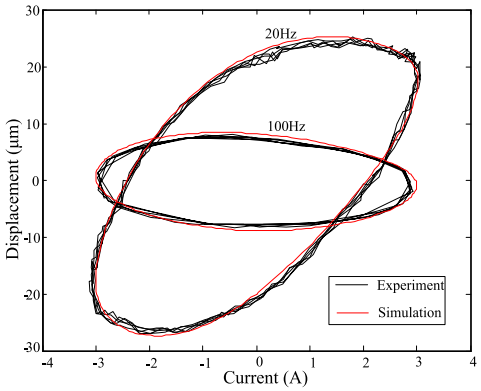

FIGURE 10. GMA model verification.

B. EXPERIMENT IN DIFFERENT CONTROL STRATEGIES

Four different algorithms (DIM, FPD, FCFPD and LFCFPD) are respectively applied in the GMA control system under complex dynamic environment. In order to evaluate the tracking feature of these control methods, the root mean square error (30) and maximum error rate (31) are introduced.

$$S_{\text{sqr}} = \sqrt{\frac{\sum_{i=1}^{n} (x_{Si} - x_{Ii})^2}{n}} \tag{34}$$

where x_{Si} is displacement sampling, x_{Ii} is displacement instruction, and n is sampling number.

$$E = \frac{|\max(x_{Si} - x_{Ii})|}{x_{\text{Amp}}} \quad (i = 1 \cdots n) \tag{35}$$

where x_{Amp} is the amplitude of displacement instructions.

In order to evaluate the control algorithms, these four controllers use the same control parameters. The controller parameters are composed of model parameters and FPD parameters. The model parameters in Tab.2 are adopted for the DIM, FCFPD and LFCFPD controller. The FPD parameters contain fuzzy control rule, K_{p} and K_{d}, which are adopted for the FPD, FCFPD and LFCFPD controller. The fuzzy control rule is in Tab.1, K_{p} is 1.25, and K_{d} is 0.136.

When the input is $8\sin(40\pi t) + 0.5\sin(200\pi t) + 0.5\sin(400\pi t)$ in 40kg load, the response curves are shown in Fig.11. The response times of FPD and DIM are obviously lower than LFCFPD and FCFPD in complex frequency and heavy load. The root mean square errors are 1.807, 2.677, 1.275, 0.332 and maximum error rates are 30.66%, 56.44%, 26.89%, 7.12% when control algorithms are respectively DIM, FPD, FCFPD and LFCFPD. The root mean square error of FCFPD is 3.84 times and maximum error rate is 3.78 times larger than LFCFPD. LFCFPD achieves higher tracking accuracy comparing with FCFPD in mixture of frequencies and large load tracking. This is because Lyapunov direct method improves the robustness of system through choosing appropriate control parameters. Therefore, LFCFPD can improve response speed by feed-forward compensation based on inverse model, resist random noise and model error disturbance by fuzzy PD and enhance the robustness by Lyapunov direct method.

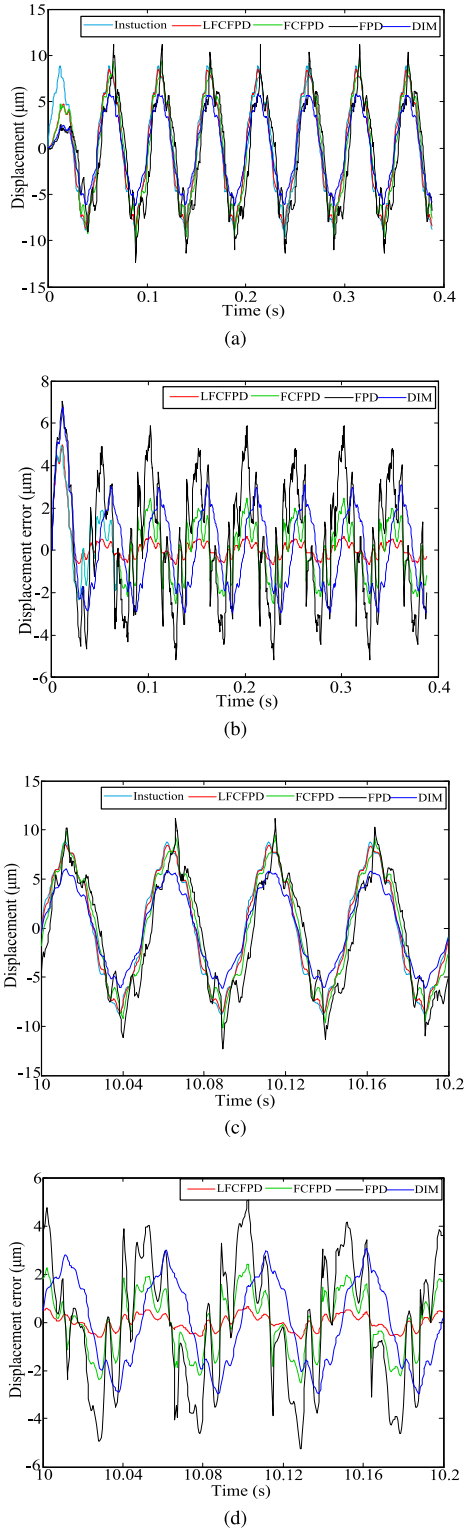

FIGURE 11. Response in different control algorithms. (a) Transient response curves of displacement. (b) Transient response curves of displacement error. (c) Steady-state response curves of displacement. (d) Steady-state response curves of displacement error.

V. CONCLUSION

Lyapunov direct method that is integrated inverse model feed-forward compensation fuzzy PD control can effectively improve the dynamic output features, reduce the root mean square error from 1.275 to 0.332 and maximum error rate from 26.89% to 7.12%, which can draw following conclusions:

1. Lyapunov direct method that is integrated into inverse model feed-forward compensation fuzzy PD control can improve the dynamic output feature especially in some complex environments.

2. LFCFPD can improve response speed by feed-forward compensation based on inverse model, resist random noise and model error disturbance by fuzzy PD and enhance the robustness by Lyapunov direct method.

REFERENCES

[1] S. H. Cho, H. W. Kim, and Y. Y. Kim, "Megahertz-range guided pure torsional wave transduction and experiments using a magnetostrictive transducer," *IEEE Trans. Ultrason., Ferroelectr., Freq. Control*, vol. 57, no. 5, pp. 1225–1229, May 2010.

[2] S. Karunanidhia and M. Singaperumalb, "Design, analysis and simulation of magnetostrictive actuator and its application to high dynamic servo valve," *Sens. Actuators A, Phys.*, vol. 157, no. 2, pp. 185–197, Feb. 2010.

[3] F. Braghin, S. Cinquemani, and F. Resta, "A low frequency magnetostrictive inertial actuator for vibration control," *Sens. Actuators A, Phys.*, vol. 180, pp. 67–74, Jun. 2012.

[4] Q. Liping and S. Xinchun, "Perturbation solution for vibration of magnetostrictive actuator," *Eng. Mech.*, vol. 26, no. 8, pp. 223–227, 2008.

[5] L. Lin, X. Zheng, and J. Xuzhen, "Parametric vibration in magnetostrictive actuator," *Acta Aeronaut. Astronaut. Sinica*, vol. 34, no. 10, pp. 2424–2433, Jan. 2013.

[6] U-X. Tan. W. T. Latt, C. Y. Shee, C. N. Riviere, and W. T. Ang, "Feedforward controller of Ill-conditioned hysteresis using singularity-free Prandtl–Ishlinskii model," *IEEE/ASME Trans. Mechatronics*, vol. 14, no. 5, pp. 598–605, Oct. 2009.

[7] Z. Li, C.-Y. Su, and X. Chen, "Modeling and inverse adaptive control of asymmetric hysteresis systems with applications to magnetostrictive actuator," *Control Eng. Pract.*, no. 33, pp. 148–160, Dec. 2014.

[8] A. Meng, J. Yang, M. Li, and S. Jiang, "Research on hysteresis compensation control of GMM," *Nonlinear Dyn.*, vol. 82, nos. 1–2, pp. 161–167, Jan. 2006.

[9] L. Wang, J. B. Tan, and Y. T. Liu, "Research on giant magnetostrictive micro-displacement actuator with self-adaptive control algorithm," *J. Phys., Conf. Ser.*, vol. 13, no. 13, p. 446, 2005.

[10] T. Hilgert, L. Vandevelde, and J. Melkebeek, "Neural-network-based model for dynamic hysteresis in the magnetostriction of electrical steel under sinusoidal induction," *IEEE Trans. Magn.*, vol. 43, no. 8, pp. 3462–3466, Aug. 2007.

[11] W. S. Oates and C. R. Smith, "Nonlinear optimal control techniques for vibration attenuation using magnetostrictive actuators," *J. Intell. Mater. Syst. Struct.*, vol. 19, no. 2, pp. 193–209, Feb. 2008.

[12] Y. L. S. Jingjun, "Position tracking control of magnetostrictive actuator using improved PSO algorithm," *J. Wuhan Univ. Technol.*, vol. 36, no. 6, pp. 735–742, 2014.

[13] C. Yu, C. Wang, H. Deng, T. He, and P. Mao, "Hysteresis nonlinearity modeling and position control for a precision positioning stage based on a giant magnetostrictive actuator," *RSC Adv.*, vol. 6, no. 64, pp. 59468–59476, 2016.

[14] Z. Yang, Z. He, D. Li, J. Yu, X. Cui, and Z. Zhao, "Direct drive servo valve based on magnetostrictive actuator: Multi-coupled modeling and its compound control strategy," *Sens. Actuators A, Phys.*, vol. 23, pp. 118–130, Nov. 2015.

[15] X. X. Li, W. Wang, J. H. Chen, and Z. C. Chen, "Hysteresis compensation of giant magnetostrictive actuator based on Jiles-Atherton model," *Opt. Precis. Eng.*, vol. 15, no. 10, pp. 1558–1562, 2007.

[16] D. C. Jiles and D. L. Atherton, "Theory of the magnetisation process in ferromagnets and its application to the magnetomechanical effect," *J. Phys. D, Appl. Phys.*, no. 17, no. 6, pp. 1265–1281, Nov. 2000.

[17] D. C. Jiles and D. L. Atherton, "Theory of ferromagnetic hysteresi," *J. Magn. Magn. Mater.*, vol. 6, nos. 1–2, pp. 48–53, Sep. 1986.

[18] D. C. Jiles, "Dynamics of domain magnetization and the Barkhausen effect," *Czechoslovak J. Phys.*, vol. 50, no. 8, pp. 893–924, Aug. 2000.

[19] F. T. Calkins, R. C. Smith, and A. B. Flatau, "Energy-based hysteresis model for magnetostrictive transducers," *IEEE Trans. Magn.*, vol. 36, no. 2, pp. 429–439, Mar. 2000.

[20] D. C. Jiles, *Introduction to Magnetism and Magnetic Materials*. New York, NY, USA: Chapman & Hall, 1991.

[21] J. Zhenyuan, W. Xiaoyi, and W. Fuji, "Parameters identification method of giant magnetostrictive actuators," *Chin. J. Mech. Eng.*, vol. 43, no. 10, pp. 9–13, 2007.

[22] R. Aissa, G. Kamel, H. Boualem, and B. Hemici, "Design of an optimized fractional order fuzzy PID controller for a piezoelectric actuator," *Control Eng. Appl. Inform.*, vol. 17, no. 3, pp. 41–49, Sep. 2015.

[23] L. Guokang and Y. Shen, "Fuzzy-reasoning based self-tuning PID control for ultra-magnetostriction micro-displacement," *Mech. Sci. Technol. Aerosp. Eng.*, vol. 30, no. 6, pp. 1025–1032, 2011.

[24] A. M. Lyapunov, *The General Problem of Stability of Motions*. Moscow, Russia: Fizmatgiz Press, 1950.

[25] X. Gao and Y. Liu, "Parameter identification based on modified simulated annealing differential evolution algorithm for giant magnetostrictive actuator," *AIP Adv.*, vol. 8, no. 1, Jan. 2018, Art. no. 015002.

XIAOHUI GAO received the B.S. degree in mechanical engineering from the Hebei University of Architecture, Hebei, China, in 2010, and the Ph.D. degree in mechatronic engineering from Beihang University, Beijing, China, in 2016, where he is currently pursuing the Ph.D. degree in mobile station in electric engineering. His research interests include hydraulic servo control, smart material actuator, and nonlinear control.

YONGGUANG LIU received the Ph.D. degree in mechanical engineering from the Harbin University of Technology, Harbin, China, in 1994 and 1999. He was a Postdoctoral Research with Tsinghua University, from 1999 to 2002. He has been with the School of Automation Science and Electrical Engineering, Beihang University, as an Associate Professor. His research interests include hydraulic servo control, industrial robots, smart material actuator, and nonlinear active vibration control.